Geophysical Research Letters

RESEARCH LETTER
10.1029/2023GL105258

Sensitivity of Rainfall Extremes to Unprecedented Indian Ocean Dipole Events

David MacLeod[1], Erik W. Kolstad[2], Katerina Michaelides[3,4,5], and Michael Bliss Singer[1,4,6]

[1]School of Earth and Environmental Sciences, Cardiff University, Cardiff, UK, [2]NORCE Norwegian Research Center, Bjerknes Center for Climate Research, Bergen, Norway, [3]School of Geographical Sciences, University of Bristol, Bristol, UK, [4]Earth Research Institute, University of California, Santa Barbara, Santa Barbara, CA, USA, [5]Cabot Institute for the Environment, University of Bristol, Bristol, UK, [6]Water Research Institute, Cardiff University, Cardiff, UK

Key Points:

- Unprecedented strong positive Indian Ocean Dipole (IOD) events are likely to bring extreme rainfall to East Africa
- The extreme component of the seasonal distribution of rain days is particularly sensitive to the magnitude of the IOD
- The impact of larger IOD events on extreme rainfall frequency increases non-linearly with the IOD magnitude

Supporting Information:

Supporting Information may be found in the online version of this article.

Correspondence to:

D. MacLeod,
macleodd1@cardiff.ac.uk

Citation:

MacLeod, D., Kolstad, E. W., Michaelides, K., & Singer, M. B. (2024). Sensitivity of rainfall extremes to unprecedented Indian Ocean Dipole events. *Geophysical Research Letters*, *51*, e2023GL105258. https://doi.org/10.1029/2023GL105258

Received 10 JUL 2023
Accepted 9 JAN 2024

Abstract Strong positive Indian Ocean Dipole (pIOD) events like those in 1997 and 2019 caused significant flooding in East Africa. While future projections indicate an increase in pIOD events, limited historical data hinders a comprehensive understanding of these extremes, particularly for unprecedented events. To overcome this we utilize a large ensemble of seasonal reforecast simulations, which show that regional rainfall continues to increase with pIOD magnitude, with no apparent limit. In particular we find that extreme rain days are highly sensitive to the pIOD index and their seasonal frequency increases super-linearly with higher pIOD magnitudes. It is vital that socio-economic systems and infrastructure are able to handle not only the increasing frequency of events like 1997 and 2019 but also unprecedented seasons of extreme rainfall driven by as-yet-unseen pIOD events. Future studies should prioritize understanding the hydrological implications and population exposure to these unprecedented extremes in East Africa.

Plain Language Summary The Indian Ocean Dipole is a pattern of climate variability in the Indian Ocean, characterized by opposite-signed sea surface temperature differences from normal in the west and east. During positive events (pIOD), the western Indian Ocean is warmer than usual, which disrupts the normal circulation of the atmosphere. When pIOD is strong, extreme rainfall and flooding are common in East Africa. This happened in 1997 and 2019. According to future predictions, the frequency of extreme pIOD events will increase. However, our understanding of these events is limited as there is not a large enough sample of past events in the historical data to study. To address this, we evaluate a large collection of climate model simulations called seasonal reforecasts. The results show no evidence of an upper limit to the impact of pIOD on regional rainfall. The frequency of rain days increases during pIOD, whilst extremely heavy rain days increase even more. This means that more frequent extreme pIOD seasons will likely bring more heavy rainfall impacts. It also means that if pIOD reaches a high magnitude which has not yet been recorded, the rainfall impacts are likely to be even larger than those seen in 1997 or 2019.

1. Introduction

The population of East Africa is exposed to numerous climate hazards which are projected to be exacerbated by climate change in the future: drought (Haile et al., 2019), heat stress (Rahimi et al., 2021) and extreme rainfall associated with flooding (Wainwright et al., 2021) are increasing in magnitude and frequency in the East Africa region and negatively impact lives, livelihoods, socio-economic development, and ecosystems. Creating plausible future climate scenarios assists in addressing these threats by offering a framework to ensure that disaster response plans and funding are adequate to meet the hazard challenges.

The future of rainfall over East Africa is a subject of ongoing research and debate. A key uncertainty arises from an inconsistency between climate model projections and recent observed trends in rainfall. This is known as the "East Africa Climate Paradox" in which climate models generally project a wetter future for the region, while recent observations indicate a drying trend (Rowell et al., 2015). This discrepancy has raised concerns about the reliability of climate models, which frequently fail to accurately represent key characteristics and trends of regional rainfall and the processes which influence it (Ahn et al., 2017; Ayugi et al., 2021; Tierney et al., 2015). A cautious and critical approach when using climate model output over East Africa is therefore essential, particularly regarding rainfall projections. Naive use of model outputs without consideration of other sources of information such as historical observations and the processes which drive climate variability is likely to lead to inappropriate

decisions being made. Observations and physical understanding are key to constrain model output and produce reliable projections of future climate.

To better address uncertainties in climate projections, the novel "storyline" approach has gained traction as an alternative to the traditional "risk-based" approach (Shepherd et al., 2018). The approach focuses on developing plausible narratives that capture the range of possible changes in climate drivers and their associated impacts in the regional expression of climate. By exploring physically consistent changes in these climate drivers, scientists and stakeholders can better understand the potential consequences and plan for plausible future impacts of climate change.

One key driver of interannual variability in East African rainfall is the Indian Ocean Dipole (IOD), which has a strong and extensively studied teleconnection to the region's short rains season, generally occurring from October to December (hereafter OND) (Black et al., 2003; Kolstad & MacLeod, 2022; MacLeod et al., 2021; Ogwang et al., 2015; Owiti et al., 2008). Positive IOD events (hereafter pIOD) have warmer-than-normal temperatures in the west Indian Ocean and cooler ocean temperatures near Indonesia (Saji et al., 1999). These events subvert the normal Walker Circulation over the region through a weakening both near-surface westerlies over the Indian Ocean and subsidence over East Africa (Saji & Yamagata, 2003). During pIOD events there is increased convection (MacLeod et al., 2021), more rainfall and a risk of flooding, as seen in the strong pIOD years of 1997 and 2019 (Latif et al., 1999; Wainwright et al., 2021). El Niño is also noted as a strong driver of wet OND seasons in East Africa. However, it has been shown that its influence on rainfall arises through its ability to trigger pIOD events, such as in 1997 (Kolstad & MacLeod, 2022; MacLeod et al., 2021). When a strong El Niño has occurred without a strong pIOD the impact on the short rains has been moderate, such as in 2015 (MacLeod & Caminade, 2019), and significantly smaller than the very wet season during pIOD events that occur independently of El Niño, such as in 2019 (Wainwright et al., 2021).

Evaluation of tropical climate dynamics in coupled climate model projections suggests that pIOD frequency will increase in the future (Cai et al., 2014), particularly in terms of extreme pIOD events compared to moderate pIOD events (Cai et al., 2021). During pIOD events the impacts on Indian Ocean climate are most significant, and can even lead to reversals of the normal direction of atmospheric flow over the Indian Ocean such as seen in 2019 (Wainwright et al., 2021). Based on historical records of pIOD impacts, more frequent pIODs can lead to more frequent seasons of extremely high rainfall totals in East Africa during OND, as well as more instances of extreme shorter-duration rainfall events within those seasons. However, due to the small number of extreme pIODs in the satellite record of rainfall observations and limited availability of gauge data, it remains challenging to robustly infer the plausible range of seasonal extreme rainfall outcomes during pIOD. In particular, it is unclear if extreme pIOD will have differing impacts on the frequency of extreme rainfall days compared to more moderate days. This is a question of crucial importance; aside from increasing flood risk, increasing seasonal frequency of extreme rain days has negative impacts on agriculture (Shortridge, 2019) and economic production (Kotz et al., 2022), yet it may lead to increased rates of groundwater recharge (Adloff et al., 2022; Seddon et al., 2021). Understanding what to expect from future extreme IOD events is a priority.

In this study our starting point is the plausible storyline that extreme IOD events will increase in future (Cai et al., 2014, 2021). We then leverage the large amount of data available from initialized seasonal reforecasts to explore plausible rainfall responses to extreme pIOD. Such reforecasts provide a large number of simulations from which infrequent events can be more robustly sampled, as first demonstrated by Van den Brink et al. (2004). Pooling these seasonal reforecasts provides many more instances of extreme pIOD than have occurred historically, supporting a statistically robust diagnosis of the behavior of regional rainfall to extreme pIOD. In this way we bring together two new threads of climate science methodology; storylines and pooled reforecasts, opening a new line of evidence on future climate risk.

2. Data and Methodology

For rainfall, daily data from the CHIRPS v2 data set is used (C. Funk et al., 2015). CHIRPS is available from 1981 to present on a spatial grid spacing of 0.05°; here we focus on data from 1981 to 2020. CHIRPS is based on infra-red satellite measurement of cloud top temperatures, calibrated with rain gauge data. We chose the CHIRPS rainfall data set because whilst public rain gauge data sets have very low sampling density over large parts of East Africa (e.g., Menne et al. (2012)), CHIRPS incorporates data from a relatively large number of stations in the

region, unavailable in other products (Dinku et al., 2018). For each year we calculate OND seasonal total rainfall, along with the number of days in that 3-month window with daily rainfall exceeding a series of thresholds (extremes): 1 mm, 10 mm, 20 mm and 50 mm. In order to diagnose the atmospheric pathways of IOD impacts on rainfall, we also consider atmospheric circulation in parallel, using divergence and zonal winds at 200 hPa and 850 hPa from the ERA5 reanalysis (Hersbach et al., 2020).

The IOD index is based on sea surface temperatures (SSTs) over two regions of the Indian Ocean. We use the standard index first defined by (Saji et al., 1999), known as the Dipole Mode index, which is the difference in the SST anomalies averaged over a western region of the Indian Ocean (10°S to 10°N, 50°–70°E) and an eastern region (−10° to 0°S, 90–110°). We calculate the average index over the OND rainfall season based on the HadISST data set (Rayner et al., 2003), which is derived from various sources, including in-situ observations from ships, buoys and coastal stations, as well as satellite data.

To carry out pooled reforecast analysis we use the SEAS5 seasonal reforecast data (Johnson et al., 2019). SEAS5 is the operational seasonal forecasting system run by the European Centre for Medium-Range Weather Forecasts (ECMWF). Alongside the operational forecast, a reforecast data set is also available for bias-correction and skill assessment. These reforecasts are initialized on the 1st of every month from 1981 up to the start of the operational archive. Like the operational forecasts, each reforecast produces a 7-month forecast, and for each initial date an ensemble of 25 members is run (51 members are run for the operational forecast).

Here we repurpose the SEAS5 reforecast data to evaluate the sensitivity of OND seasonal rainfall to the IOD index. The monthly initialization frequency and the 7-month forecast window means that simulations of OND are present in multiple reforecast start dates: specifically the July, August, September and October initializations. We extract OND output from these four starts, for each of the 25 members and the 40 reforecast years 1981–2020. The result is a pool of 4,000 simulations of OND, on which we base the pooled-reforecast analysis. We take daily rainfall from each member at the atmospheric model spatial resolution of 36 km and calculate the same seasonal rainfall metrics as defined above. We also extract the monthly SST field associated with each reforecast member at a one-degree spatial resolution, and use it to calculate the IOD index as above. For a parallel evaluation of atmospheric circulation, we use monthly values of divergence and zonal wind at 200 and 850 hPa from the reforecast.

Reforecast pooling has a relatively long history. It was initially used to improve estimates of extreme storm surge and coastal flooding (Van den Brink et al., 2004, 2005) and has since been used to evaluate extreme wind (Breivik et al., 2014), precipitation (Kelder et al., 2020; Thompson et al., 2017) and streamflow (Brunner & Slater, 2022), and it has been used to explore surface responses to the stratospheric polar vortex (Kolstad et al., 2022). Recently, reforecast pooling has been branded as the UNprecedented Simulated Extreme ENsemble (UNSEEN) approach (Thompson et al., 2017), highlighting the potential use of the method in examining never-before-seen events.

In previous studies using reforecast pooling, only the longest lead forecasts are mainly used in the analysis and shorter lead runs tend to be discounted (e.g., Thompson et al., 2017). The rationale is to remove the influence of the initial state and generate a reforecast pool that is as close to the unforced climate system as possible, from which event likelihoods can be estimated. However, our motivation here is not to estimate probabilities, but to explore sensitivities to known forcing mechanisms. By including the shortest lead times in our pooled reforecast, we will more densely sample the state space close to the particular initial states of those short lead runs. This is an acceptable approach because all available reforecast runs are physically (internally) consistent estimates of potential IOD-rainfall behavior and are therefore appropriate to include in the pool.

Our reforecast pool consists of 4,000 simulations of OND, each with a set of rainfall metrics and a corresponding IOD index. This is about 100 times larger than the CHIRPS sample of about 40 seasons. We begin by evaluating the spatial pattern of the IOD influence on regional rainfall, in order to establish the model's ability to represent the teleconnection, along with the biases in the rainfall metrics. Following this, we evaluate the sensitivity of each rainfall metric to changes in the IOD index, focusing particularly on changes when IOD reaches extremely high levels.

3. Results

Figure 1 shows the representation of the spatial pattern of the IOD-rainfall teleconnection. For both the historical observations and the SEAS5 reforecast, the data are stratified into five equal subsets according to the IOD index

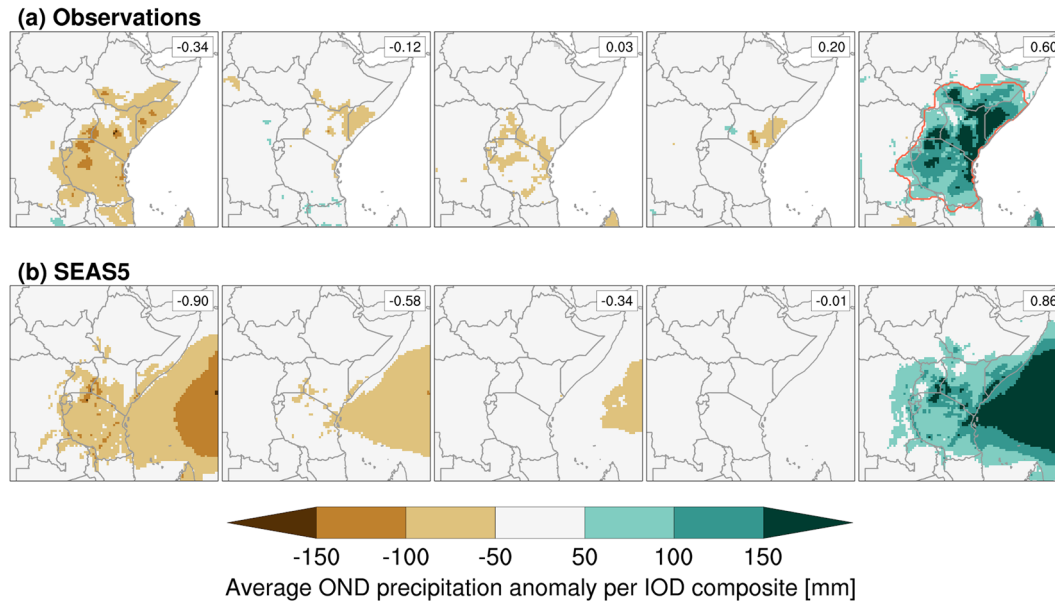

Figure 1. Mean OND rainfall anomalies in bins divided according to Indian Ocean Dipole (IOD) index for (a) observations (b) the SEAS5 reforecast. Plots are arranged from the most negative IOD composite on the far left to the most positive IOD composite on the far right, and the average IOD index for each composite is noted on the top right of each plot. The red outline in the top right panel defines a region of the core IOD rainfall teleconnection and is used for area averages in Figure 3. This region is derived from a smoothed region encompassing the areas of high rainfall in the panel. Note that CHIRPS does not have values over the ocean, unlike SEAS5.

to make a like-for-like comparison whilst keeping reasonable populations in the observational composites. For the historical observations (Figure 1a) the association between rainfall and IOD is as expected, with instances of strong positive IOD leading to large increases in seasonal total rainfall (fifth subset, average IOD index 0.6). For weakly positive IOD seasons (fourth subset, average IOD index 0.2), no notable impact on seasonal rainfall is observed. Seasons with the largest negative index value (first subset, average IOD value −0.34) lead to suppression of seasonal rainfall totals. However the magnitude of the negative anomalies for the most negative IOD seasons is significantly smaller than the magnitude of the positive anomalies for the most positive IOD seasons. This is partly because the precipitation has a hard lower limit of zero rainfall, while there is no hard upper limit.

Pooled reforecasts from SEAS5 broadly reproduce the pattern seen in the observations: enhancing rainfall only for the strongest IOD values, and with weaker negative rainfall anomalies for the most negative IOD events (Figure 1b). The corresponding impacts of the IOD on the atmospheric circulation are shown in Figures S1–S8 of Supporting Information S1 and show that positive IOD states weaken the typical Walker Circulation pattern. Increasing IOD magnitudes lead to a significant reduction in convergence at upper levels over East Africa and the western Indian Ocean, along with a change in the sign of upper-level winds westerly to easterly. In the lower troposphere an increasing IOD index results in a significant weakening of the normal westerlies in the central Indian Ocean. SEAS5 broadly reproduces these signals.

When looking more closely at the spatial impact of the IOD on rainfall across East Africa, it is clear that the simulation is imperfect. During strong positive IOD events, SEAS5 generates the largest rainfall increase over humid areas in western Kenya and the central highlands, and in a band along the coast of southern Somalia and northern Tanzania. However, the observed rainfall response to IOD shows a more widespread impact. In observations the same enhanced rainfall is seen as in SEAS5, but large increases are also apparent across semi-arid and arid regions: in northeast Kenya, southern Ethiopia, and in southern Somalia away from the coast. In consideration of potential observational uncertainty, alternative observational data sets of GPCP (Adler et al., 2018) and TAMSAT (Maidment et al., 2014) were used to diagnose the composite rainfall response. These are presented in Figure S1 of Supporting Information S1 and show a pattern of enhanced rainfall during pIOD in semi-arid and arid regions which is consistent with analysis based on CHIRPS, which is not reproduced by SEAS5. This mismatch in the spatial details of the rainfall associated with the IOD teleconnection reduces confidence that SEAS5 is able to accurately infer relative changes in rainfall during extreme IOD events at small spatial scales.

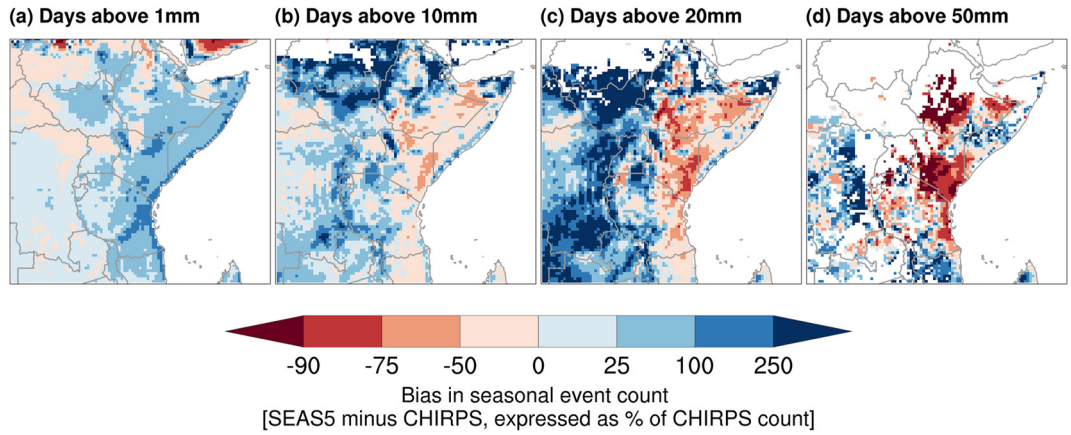

Figure 2. SEAS5 frequency bias in seasonal rainfall metrics, showing results for seasonal count of days above 1, 10, 20, and 50 mm rainfall (left to right). Bias is calculated as the difference in mean seasonal count between SEAS5 and CHIRPS rainfall, expressed as the percentage of the CHIRPS value. White shading on land is used for areas where the mean seasonal count in CHIRPS is zero (white on ocean is undefined due to lack of CHIRPS data there).

Figure 2 shows the bias in the average frequency of rain days above a range of thresholds (extremes), expressed as the frequency of days in SEAS5 minus the frequency in CHIRPS, as a percentage of the CHIRPS frequency. The pattern of bias is nonlinear and spatially complex. In particular, SEAS5 produces many more rain days greater than 1 mm than CHIRPS (Figure 2a) along the coast and inland, but further west from the coast (in western Kenya and beyond) it generates far fewer. This pattern is largely reversed for heavier rain days (above 10 and 20 mm, Figures 2b and 2c), which are overestimated relative to CHIRPS in the west, underestimated further east, but then overestimated again in a thin coastal band. For the most extreme rain days (50 mm, Figure 2d) the frequency is strongly underestimated by SEAS5 in Kenya and Ethiopia, but in parts of Somalia and Tanzania and the DRC the frequency is vastly overestimated (over 250% of the CHIRPS frequency).

The analysis presented in Figure 1 demonstrates that SEAS5 is unable to accurately reproduce the precise spatial pattern of the IOD teleconnection, whilst Figure 2 demonstrates that it does not reliably reproduce the daily distribution of seasonal rain events in these data sets. It would therefore be misguided to use the SEAS5 reforecast to attempt to precisely quantify rainfall responses to IOD, in terms of the impact on specific rainfall thresholds, and/or in terms of the spatial pattern of its impact.

Informed by this, we used the pooled reforecast to quantify impacts on the area-average response. Seasonal rainfall metrics already calculated by grid point are averaged over the spatial domain corresponding to the observed rainfall response to positive IOD events (indicated by the red outline in the final panel of Figure 1a, derived from a smoothed region encompassing the areas showing high rainfall in that figure). We also treat the precise values of seasonal event frequency with caution. By interrogating the relationship between seasonal rainfall and the IOD index, we investigate the functional form of the relationship as the IOD index approaches extreme values. Furthermore, we explore how the IOD-rainfall relationship depends on the rainfall distribution: is the same influence seen for the frequency of moderate rain days compared to extreme days, for instance.

Figure 3 shows the relationship between the IOD index and the seasonal frequency of rainfall events, in both observations and SEAS5. The sample of seasons is stratified into equally-populated bins based on the IOD index, with a different number of bins chosen for SEAS5 and observations to balance the bin size with the ability to resolve the functional relationship (10 4-member bins for observations and 100 40-member bins for SEAS5). The area-average seasonal frequency in each bin is then scaled by the frequency under neutral conditions (calculated as the frequency during all seasons with an absolute IOD index value below 0.5).

We found a clear nonlinear difference between negative and positive IOD events; for all rainfall metrics considered, the largest magnitude positive events have greater impacts on rainfall than the largest magnitude negative events. A particular sensitivity of extreme rainfall events to positive IOD can be seen, for example, with a SEAS5 IOD index of 1, resulting in a +75% increase in the frequency of days above 50 mm compared to neutral IOD conditions, whereas there is only a 30% increase for rainfall days above 10 mm (Figure 3b). Further, this

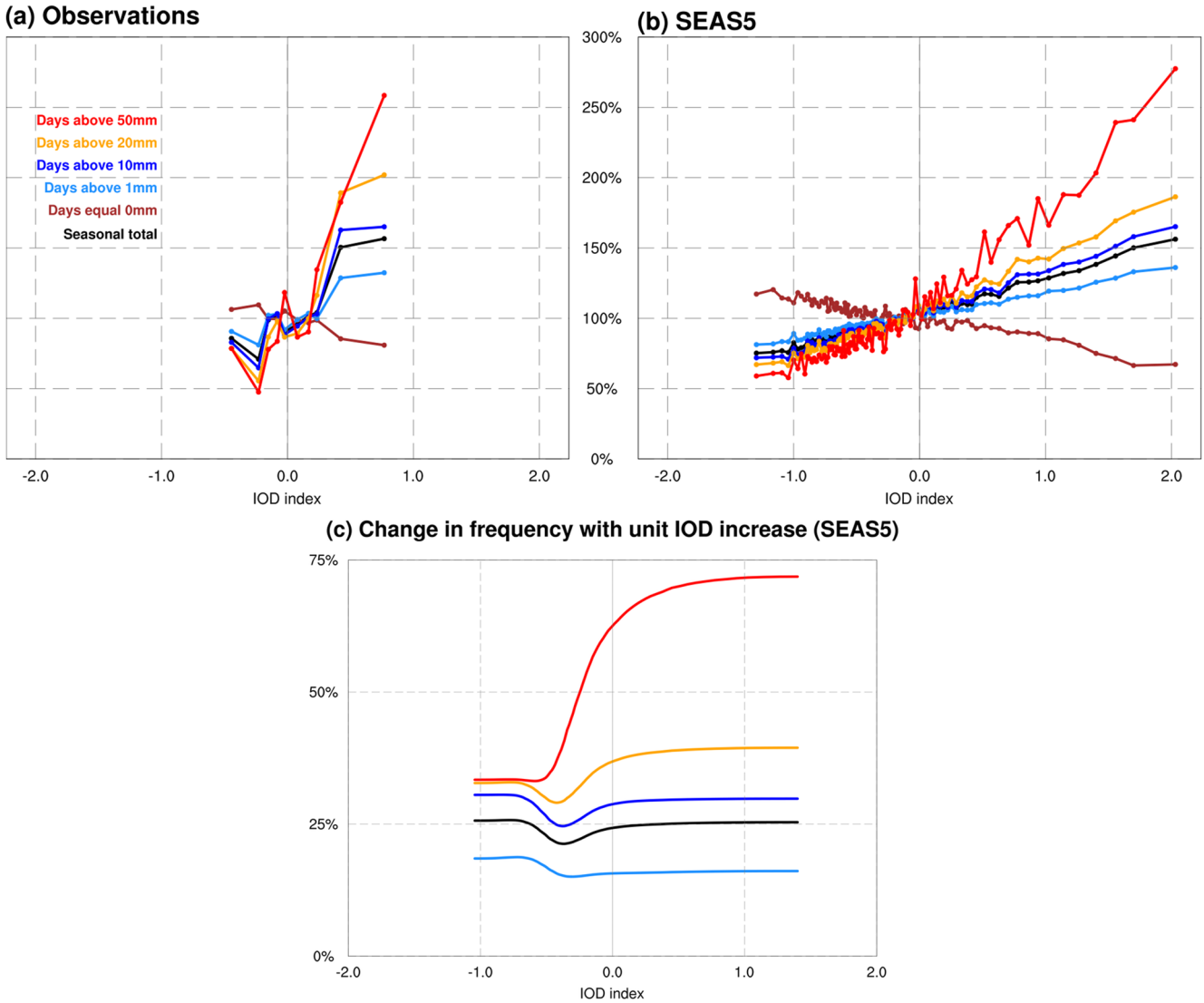

Figure 3. Relationship between seasonal rainfall metrics and Indian Ocean Dipole (IOD) index for (a) observations and (b) the SEAS5 reforecast. Data is subset into bins (10 4-member bins for CHIRPS and 100 40-member bins for SEAS5), and the area-average mean count in each bin relative to IOD-neutral conditions is plotted as a function of the mean IOD index in that bin. Panel (c) is derived from panel (b) and shows the sensitivity of changes in seasonal rainfall metrics to IOD increases as a function of IOD index (see text for details of calculation).

heterogeneous influence of the IOD on different parts of the rainfall distribution is seen in the analysis of observations, for which extreme rainfall days also show the highest sensitivity to IOD magnitude and sign. This can also be in the reforecast when evaluated for initialization months separately (not shown).

Beyond this differential impact on parts of the daily rainfall distribution, a nonlinear relationship can be seen within the frequency of extreme rain days. For an increase in the IOD index from 0 to 1, an increase in the frequency of 10 and 50 mm days of 30% and 75%, respectively, is seen. However with a further unit increase in the IOD index from 1 to 2, the 10 mm day frequency increases by a further 30%, but the frequency of 50 mm days increases dramatically by a further 100%, to 175% of the IOD-neutral value. This nonlinear functional relationship is quantified in Figure 3c, which shows the sensitivity of the seasonal frequency to a unit IOD increase. This has been calculated as the local gradient (i.e., the first derivative) of the data in Figure 3b and is smoothed by repeated application of a three-point running-average due to highly noisy signal in the negative part of the domain.

The gradients demonstrate a clearly increasing sensitivity to IOD increases for the wettest parts of the daily rainfall distribution, as well as a nonlinear relationship between IOD and extreme rainfall. For days above 1, 10,

and 20 mm, a unit increase in the IOD index leads to an average increase in seasonal frequency of +17%, +28% and +35%, and this does not change considerably across the IOD domain. By contrast, a unit increase in the IOD index increases the frequency of days over 50 mm by 34% in the negative part of the domain, rising to 72% for increases when the index is already positive. The same relationship can also be seen in the reforecast when evaluated for initialization months separately (not shown). Overall this demonstrates that positive IOD events disproportionately increase the frequency of heavy and extreme rainfall, and further unprecedented increases in IOD magnitude are likely to bring unprecedented frequencies of extreme rainfall days.

A complementary evaluation of the sensitivity of atmospheric circulation metrics to the IOD index is consistent with these findings (Figure S10 in Supporting Information S1). Additionally, this analysis demonstrates that the nonlinearity of the rainfall response to the IOD does not arise from the interaction of IOD with regional atmospheric dynamics, which are found to be linear. By deduction, this nonlinearity must arise from how linear changes in local dynamics translate to the generation of extreme rainfall. In particular, a shift from convergence to divergence in the upper atmosphere over East Africa is noted for IOD index values beyond +0.5, suggesting a discrete shift from suppression to enhancement of deep convection for positive IOD states.

4. Discussion

Using pooled reforecast data, we have demonstrated that the influence of the IOD on East African rainfall continues to grow as the magnitude of the pIOD increases. There is no evidence of a saturation effect, where increases in rainfall slow down as the IOD index continues to increase. Instead, rainfall continues to increase with increasing IOD index. In addition, higher values of the IOD index appear to have a stronger impact on the extreme end of the rainfall distribution. Over the whole distribution, some non-linearity is expected, since this is 'built-in' when considering indices that are zero-bounded: negative IOD events can only reduce the rainfall to zero, whilst the impact of positive events is effectively unbounded. However, the non-linearity observed is not simply a difference between the impact of negative and positive phases of IOD impacts but is seen in the positive phase alone, whereby the increase in rainfall between moderate to strong IOD events is significantly larger than the increase between neutral to moderate events. Evidence of similar non-linearity between the IOD and extreme rainfall events over India has also been found (Krishnaswamy et al., 2015).

Overall, our results indicate a robust relationship between extreme precipitation and pIOD. Under high-emission climate scenarios, projections have indicated that the frequency of extreme pIOD events could increase by a factor of almost three during the 21st century, from one event every 17 years to one event every 6 years by the end of the century (Cai et al., 2014). In this climate we can expect more frequent heavy seasonal rainfall and by extension, severe flooding in October-December in East Africa, such as seen in 2019 (Wainwright et al., 2021).

Our findings align with the existing understanding of the impact of the IOD on tropical circulation across the Indian Ocean (Saji & Yamagata, 2003). Whilst pIOD events weaken the normal Walker circulation, as they approach extreme levels it is physically plausible for them to reverse the circulation, as in 2019 (Wainwright et al., 2021). As pIOD events continue to intensify, reaching unprecedented magnitudes, we expect an even more pronounced reversal of the typical Walker circulation (C. C. Funk, 2021), leading to more frequent and deeper convective events which result in higher magnitudes of extreme rainfall.

Evidence presented here from rainfall and dynamical analysis suggests that positive IOD states shift the mean local dynamics from convergence in the upper atmosphere to divergence, supporting deep convection and extreme rainfall events. Further increases in the IOD to extreme levels continue to enhance upper-level divergence and the associated likelihood of deep convection, facilitating the production of even greater daily rainfall totals. It should be noted, however, that some tapering off of the IOD's influence is noted on upper-level zonal winds over East Africa. This suggests that there may be a physical limit to the IOD's influence on tropical dynamics as it reaches unprecedented levels. However, we do not detect any signal of this saturation in upper-level divergence fields or rainfall patterns.

Reflecting on the ability of the fidelity of SEAS5 rainfall, our analysis reveals some unreliability of the SEAS5 model representation of the spatial fingerprint of the IOD teleconnection when compared to the CHIRPS rainfall data set. These biases limit our ability to make definitive statements about the spatial distribution of extreme pIOD behavior. Understanding potential shifts in the spatial pattern of rainfall during extreme pIOD states is crucial, but due to a lack of confidence in the model's ability to represent these fine-scale spatial details we refrain

from utilizing this data to answer this question. Instead our confidence lies in the sign of the relationship on average over the study region: increasing pIOD will impact precipitation extremes disproportionately.

Notably, the potential extreme rainfall impacts shown here do not take future changes driven by thermodynamics into account. While SEAS5 reforecasts simulate temperature distributions consistent with recent levels of greenhouse gases, a future climate is almost guaranteed to be warmer (Ongoma et al., 2018). According to Clausius-Clapeyron scaling, a warmer atmosphere will hold more water, increasing the capacity for higher magnitude rainfall events (Pfahl et al., 2017). Indeed some evidence suggests that changes in hourly rainfall extremes in the tropics are exceeding what is expected from Clausius-Clapeyron scaling (Guerreiro et al., 2018). Combined with future increases in pIOD magnitudes and their corresponding enhancement of deep convection over East Africa, this could lead to truly unprecedented rainfall extremes over the region with potentially devastating impacts.

Looking ahead, decision-makers and regional stakeholders must prepare for the recurrence of positive pIOD events, which may have impacts comparable to or surpassing those witnessed in 1997 and 2019. The evidence presented in this study strongly advocates for a more comprehensive approach to preparedness and contingency planning, aimed at anticipating seasons marked by even more pronounced precipitation extremes than those observed during these recent high-impact years. Such extremes could potentially expand the geographical scope of flooding impacts and expose a larger portion of the population to flood risks.

Communities, government and industry should strive to create resilience to this heightened risk, which can be quantified using process-based hydrological models designed for such regions (MacLeod et al., 2023; Quichimbo et al., 2021). Yet, caution must be taken in using rainfall from climate models to drive such models, as nonlinear and spatially-dependent biases are likely to influence simulations in an opaque way. The pattern of SEAS5 found here (overestimated rain-day frequency and underestimated heavy rain-day frequency) in places is consistent with the perennial problem of "drizzle" in climate models (e.g., Piani et al., 2010), which has been linked to an overestimation of convective and underestimation of non-convective precipitation (Chen et al., 2021). This may suggest routes to improving simulations of daily rainfall in SEAS5 (although this typical "drizzle" pattern is not consistently seen everywhere in our results). In addition, we note a particular pattern of biases along coastal regions, which may be related to model representation of convection since rainfall in this region has been shown to be particularly sensitive to parameterized convection (Finney et al., 2019). Moving toward convection-resolving scales may lead to improved biases here as well.

Entirely bias-free climate model output would be highly desirable for use in hydrological and other impact models. However in its absence an alternative approach to understanding plausible future hydrological impacts involves using stochastic rainfall generation scenarios to explore the effect of changes in rainfall characteristics, such as intensity, duration and storm frequency, in a controllable and transparent manner (Singer et al., 2018). This work will be the subject of future investigation.

5. Conclusions

The storyline approach to climate change projections follows a path that outlines the implications of plausible future changes in key climate drivers. One such driver of East African rainfall is the IOD, for which extreme positive events have been projected to increase in frequency. Here we have taken this scenario as a plausible future for the region, and using the technique of pooling seasonal reforecasts we examine the potential impact of this kind of event on regional rainfall distribution. We find no saturation of the potential impact of the IOD on rainfall, with unprecedented pIOD events likely to lead to unprecedented seasonal rainfall totals. We also find the strongest impacts on the frequency of extreme rain days, and we find a non-linear impact such that increases in pIOD at the high end of its range have the largest impacts. Decision-makers should prepare for flooding events like 1997 and 2019 to recur, with potentially unprecedented frequency of extreme rainfall. Exploring the hydrological impacts of these unprecedented extreme seasons is a priority for future work.

In closing we note that at the time of writing this article a pIOD event has emerged in the Indian Ocean, associated with a strong El Niño event already in progress. Eighty-five percent likelihood of above-normal rainfall has been forecast for East Africa, an unprecedented level of certainty (ICPAC, 2023). Considering the record-breaking temperatures observed in 2023 so far, driven both by El Niño and global warming (WMO, 2023), it is plausible that this season may experience unprecedented levels of rainfall, resulting from the combined effect of a strong

pIOD with Clausius-Clapeyron scaling. Notably this hazard is unfolding in a region with eroded resilience from a 3-year drought (WFP, 2023), amplifying the risks to both lives and livelihoods. Based on the results of this paper we therefore anticipate severe rainfall impacts in the upcoming season, noting that these may just foreshadow the future of climate risk for East Africa.

Data Availability Statement

The CHIRPS data (C. Funk et al., 2015) are available from the Climate Hazards Center at the University of Santa Barbara, USA at https://www.chc.ucsb.edu/data/chirps. HadISST data (Rayner et al., 2003) are available from the UK Met Office Hadley Centre https://www.metoffice.gov.uk/hadobs/hadisst/. SEAS5 reforecast and ERA5 reanalysis data is available from the Copernicus Climate Data Store (Copernicus Climate Change Service, 2018; Hersbach et al., 2023).

Acknowledgments
The research was supported by funding from the European Union's Horizon 2020 program through the DOWN2EARTH and CONFER projects (Grants 869550 and 869730).

References

Adler, R. F., Sapiano, M. R., Huffman, G. J., Wang, J.-J., Gu, G., Bolvin, D., et al. (2018). The Global Precipitation Climatology Project (GPCP) monthly analysis (new version 2.3) and a review of 2017 global precipitation. *Atmosphere*, *9*(4), 138. https://doi.org/10.3390/atmos9040138

Adloff, M., Singer, M. B., MacLeod, D. A., Michaelides, K., Mehrnegar, N., Hansford, E., et al. (2022). Sustained water storage in Horn of Africa drylands dominated by seasonal rainfall extremes. *Geophysical Research Letters*, *49*(21), e2022GL099299. https://doi.org/10.1029/2022gl099299

Ahn, M.-S., Kim, D., Sperber, K. R., Kang, I.-S., Maloney, E., Waliser, D., & Hendon, H. (2017). MJO simulation in CMIP5 climate models: MJO skill metrics and process-oriented diagnosis. *Climate Dynamics*, *49*(11–12), 4023–4045. https://doi.org/10.1007/s00382-017-3558-4

Ayugi, B., Zhihong, J., Zhu, H., Ngoma, H., Babaousmail, H., Rizwan, K., & Dike, V. (2021). Comparison of CMIP6 and CMIP5 models in simulating mean and extreme precipitation over East Africa. *International Journal of Climatology*, *41*(15), 6474–6496. https://doi.org/10.1002/joc.7207

Black, E., Slingo, J., & Sperber, K. R. (2003). An observational study of the relationship between excessively strong short rains in coastal East Africa and Indian Ocean SST. *Monthly Weather Review*, *131*(1), 74–94. https://doi.org/10.1175/1520-0493(2003)131<0074:aosotr>2.0.co;2

Breivik, Ø., Aarnes, O. J., Abdalla, S., Bidlot, J.-R., & Janssen, P. A. (2014). Wind and wave extremes over the world oceans from very large ensembles. *Geophysical Research Letters*, *41*(14), 5122–5131. https://doi.org/10.1002/2014gl060997

Brunner, M. I., & Slater, L. J. (2022). Extreme floods in Europe: Going beyond observations using reforecast ensemble pooling. *Hydrology and Earth System Sciences*, *26*(2), 469–482. https://doi.org/10.5194/hess-26-469-2022

Cai, W., Santoso, A., Wang, G., Weller, E., Wu, L., Ashok, K., et al. (2014). Increased frequency of extreme Indian Ocean Dipole events due to greenhouse warming. *Nature*, *510*(7504), 254–258. https://doi.org/10.1038/nature13327

Cai, W., Yang, K., Wu, L., Huang, G., Santoso, A., Ng, B., et al. (2021). Opposite response of strong and moderate positive Indian Ocean Dipole to global warming. *Nature Climate Change*, *11*(1), 27–32. https://doi.org/10.1038/s41558-020-00943-1

Chen, D., Dai, A., & Hall, A. (2021). The convective-to-total precipitation ratio and the "drizzling" bias in climate models. *Journal of Geophysical Research: Atmospheres*, *126*(16), e2020JD034198. https://doi.org/10.1029/2020jd034198

Copernicus Climate Change Service, C. D. S. (2018). Seasonal forecast anomalies on single levels [Dataset]. Copernicus Climate Change Service (C3S) Climate Data Store (CDS). https://doi.org/10.24381/cds.7e37c951

Dinku, T., Funk, C., Peterson, P., Maidment, R., Tadesse, T., Gadain, H., & Ceccato, P. (2018). Validation of the CHIRPS satellite rainfall estimates over eastern Africa. *Quarterly Journal of the Royal Meteorological Society*, *144*(S1), 292–312. https://doi.org/10.1002/qj.3244

Finney, D. L., Marsham, J. H., Jackson, L. S., Kendon, E. J., Rowell, D. P., Boorman, P. M., et al. (2019). Implications of improved representation of convection for the East Africa water budget using a convection-permitting model. *Journal of Climate*, *32*(7), 2109–2129. https://doi.org/10.1175/jcli-d-18-0387.1

Funk, C., Peterson, P., Landsfeld, M., Pedreros, D., Verdin, J., Shukla, S., et al. (2015). The climate hazards infrared precipitation with stations—A new environmental record for monitoring extremes. *Scientific Data*, *2*(1), 1–21. https://doi.org/10.1038/sdata.2015.66

Funk, C. C. (2021). *Drought, flood, fire: How climate change contributes to catastrophes*. Cambridge University Press. https://doi.org/10.1017/9781108885348

Guerreiro, S. B., Fowler, H. J., Barbero, R., Westra, S., Lenderink, G., Blenkinsop, S., et al. (2018). Detection of continental-scale intensification of hourly rainfall extremes. *Nature Climate Change*, *8*(9), 803–807. https://doi.org/10.1038/s41558-018-0245-3

Haile, G. G., Tang, Q., Sun, S., Huang, Z., Zhang, X., & Liu, X. (2019). Droughts in East Africa: Causes, impacts and resilience. *Earth-Science Reviews*, *193*, 146–161. https://doi.org/10.1016/j.earscirev.2019.04.015

Hersbach, H., Bell, B., Berrisford, P., Hirahara, S., Horányi, A., Muñoz-Sabater, J., et al. (2020). The ERA5 global reanalysis. *Quarterly Journal of the Royal Meteorological Society*, *146*(730), 1999–2049. https://doi.org/10.1002/qj.3803

Hersbach, H., Bell, B., Berrisford, P., Hirahara, S., Horányi, A., Muñoz-Sabater, J., et al. (2023). ERA5 monthly averaged data on pressure levels from 1940 to present [Dataset]. Copernicus Climate Change Service (C3S) Climate Data Store (CDS). https://doi.org/10.24381/cds.6860a573

ICPAC. (2023). *Technical statement from the 65th Greater Horn of Africa Climate Outlook Forum (GHACOF65) 22 August 2023; Nairobi, Kenya* (Technical Report). IGAD Climate Prediction and Application Center. Retrieved from https://www.icpac.net/publications/statement-from-the-65th-greater-horn-of-africa-climate-outlook-forum-ghacof65-22-august-2023-nairobi-kenya/

Johnson, S. J., Stockdale, T. N., Ferranti, L., Balmaseda, M. A., Molteni, F., Magnusson, L., et al. (2019). SEAS5: The new ECMWF seasonal forecast system. *Geoscientific Model Development*, *12*(3), 1087–1117. https://doi.org/10.5194/gmd-12-1087-2019

Kelder, T., Müller, M., Slater, L., Marjoribanks, T., Wilby, R., Prudhomme, C., et al. (2020). Using unseen trends to detect decadal changes in 100-year precipitation extremes. *npj Climate and Atmospheric Science*, *3*(1), 47. https://doi.org/10.1038/s41612-020-00149-4

Kolstad, E. W., Lee, S. H., Butler, A. H., Domeisen, D. I. V., & Wulff, C. O. (2022). Diverse surface signatures of stratospheric polar vortex anomalies. *Journal of Geophysical Research: Atmospheres*, *127*(20), e2022JD037422. https://doi.org/10.1029/2022JD037422

Kolstad, E. W., & MacLeod, D. (2022). Lagged oceanic effects on the East African short rains. *Climate Dynamics*, *59*(3–4), 1043–1056. https://doi.org/10.1007/s00382-022-06176-6

Kotz, M., Levermann, A., & Wenz, L. (2022). The effect of rainfall changes on economic production. *Nature*, *601*(7892), 223–227. https://doi.org/10.1038/s41586-021-04283-8

Krishnaswamy, J., Vaidyanathan, S., Rajagopalan, B., Bonell, M., Sankaran, M., Bhalla, R., & Badiger, S. (2015). Non-stationary and non-linear influence of ENSO and Indian Ocean Dipole on the variability of Indian monsoon rainfall and extreme rain events. *Climate Dynamics*, *45*(1–2), 175–184. https://doi.org/10.1007/s00382-014-2288-0

Latif, M., Dommenget, D., Dima, M., & Grötzner, A. (1999). The role of Indian Ocean sea surface temperature in forcing East African rainfall anomalies during December–January 1997/98. *Journal of Climate*, *12*(12), 3497–3504. https://doi.org/10.1175/1520-0442(1999)012<3497:troios>2.0.co;2

MacLeod, D., & Caminade, C. (2019). The moderate impact of the 2015 El Niño over East Africa and its representation in seasonal reforecasts. *Journal of Climate*, *32*(22), 7989–8001. https://doi.org/10.1175/jcli-d-19-0201.1

MacLeod, D., Graham, R., O'Reilly, C., Otieno, G., & Todd, M. (2021). Causal pathways linking different flavours of ENSO with the Greater Horn of Africa short rains. *Atmospheric Science Letters*, *22*(2), e1015. https://doi.org/10.1002/asl.1015

MacLeod, D., Quichimbo, E. A., Michaelides, K., Asfaw, D. T., Rosolem, R., Cuthbert, M. O., et al. (2023). Translating seasonal climate forecasts into water balance forecasts for decision making. *PLOS Climate*, *2*(3), e0000138. https://doi.org/10.1371/journal.pclm.0000138

Maidment, R. I., Grimes, D., Allan, R. P., Tarnavsky, E., Stringer, M., Hewison, T., et al. (2014). The 30 year TAMSAT African rainfall climatology and time series (TARCAT) data set. *Journal of Geophysical Research: Atmospheres*, *119*(18), 10–619. https://doi.org/10.1002/2014jd021927

Menne, M. J., Durre, I., Vose, R. S., Gleason, B. E., & Houston, T. G. (2012). An overview of the global historical climatology network-daily database. *Journal of Atmospheric and Oceanic Technology*, *29*(7), 897–910. https://doi.org/10.1175/jtech-d-11-00103.1

Ogwang, B. A., Ongoma, V., Xing, L., & Ogou, K. F. (2015). Influence of Mascarene high and Indian Ocean dipole on East African extreme weather events. *Geographica Pannonica*, *19*(2), 64–72. https://doi.org/10.5937/geopan1502064o

Ongoma, V., Chen, H., Gao, C., Nyongesa, A. M., & Polong, F. (2018). Future changes in climate extremes over equatorial East Africa based on CMIP5 multimodel ensemble. *Natural Hazards*, *90*(2), 901–920. https://doi.org/10.1007/s11069-017-3079-9

Owiti, Z., Ogallo, L. A., & Mutemi, J. (2008). Linkages between the Indian Ocean Dipole and East African seasonal rainfall anomalies. *Journal of Kenya Meteorological Society*, *2*(1–2), 3–16.

Pfahl, S., O'Gorman, P. A., & Fischer, E. M. (2017). Understanding the regional pattern of projected future changes in extreme precipitation. *Nature Climate Change*, *7*(6), 423–427. https://doi.org/10.1038/nclimate3287

Piani, C., Haerter, J., & Coppola, E. (2010). Statistical bias correction for daily precipitation in regional climate models over Europe. *Theoretical and Applied Climatology*, *99*(1–2), 187–192. https://doi.org/10.1007/s00704-009-0134-9

Quichimbo, E. A., Singer, M. B., Michaelides, K., Hobley, D. E., Rosolem, R., & Cuthbert, M. O. (2021). DRYP 1.0: A parsimonious hydrological model of dryland partitioning of the water balance. *Geoscientific Model Development*, *14*(11), 6893–6917. https://doi.org/10.5194/gmd-14-6893-2021

Rahimi, J., Mutua, J. Y., Notenbaert, A. M., Marshall, K., & Butterbach-Bahl, K. (2021). Heat stress will detrimentally impact future livestock production in East Africa. *Nature Food*, *2*(2), 88–96. https://doi.org/10.1038/s43016-021-00226-8

Rayner, N., Parker, D. E., Horton, E., Folland, C. K., Alexander, L. V., Rowell, D., et al. (2003). Global analyses of sea surface temperature, sea ice, and night marine air temperature since the late nineteenth century. *Journal of Geophysical Research*, *108*(D14), 4407. https://doi.org/10.1029/2002jd002670

Rowell, D. P., Booth, B. B., Nicholson, S. E., & Good, P. (2015). Reconciling past and future rainfall trends over East Africa. *Journal of Climate*, *28*(24), 9768–9788. https://doi.org/10.1175/jcli-d-15-0140.1

Saji, N., Goswami, B. N., Vinayachandran, P., & Yamagata, T. (1999). A dipole mode in the tropical Indian Ocean. *Nature*, *401*(6751), 360–363. https://doi.org/10.1038/43854

Saji, N., & Yamagata, T. (2003). Possible impacts of Indian Ocean Dipole mode events on global climate. *Climate Research*, *25*(2), 151–169. https://doi.org/10.3354/cr025151

Seddon, D., Kashaigili, J. J., Taylor, R. G., Cuthbert, M. O., Mwihumbo, C., & MacDonald, A. M. (2021). Focused groundwater recharge in a tropical dryland: Empirical evidence from central, semi-arid Tanzania. *Journal of Hydrology: Regional Studies*, *37*, 100919. https://doi.org/10.1016/j.ejrh.2021.100919

Shepherd, T. G., Boyd, E., Calel, R. A., Chapman, S. C., Dessai, S., Dima-West, I. M., et al. (2018). Storylines: An alternative approach to representing uncertainty in physical aspects of climate change. *Climatic Change*, *151*(3–4), 555–571. https://doi.org/10.1007/s10584-018-2317-9

Shortridge, J. (2019). Observed trends in daily rainfall variability result in more severe climate change impacts to agriculture. *Climatic Change*, *157*(3–4), 429–444. https://doi.org/10.1007/s10584-019-02555-x

Singer, M. B., Michaelides, K., & Hobley, D. E. (2018). Storm 1.0: A simple, flexible, and parsimonious stochastic rainfall generator for simulating climate and climate change. *Geoscientific Model Development*, *11*(9), 3713–3726. https://doi.org/10.5194/gmd-11-3713-2018

Thompson, V., Dunstone, N. J., Scaife, A. A., Smith, D. M., Slingo, J. M., Brown, S., & Belcher, S. E. (2017). High risk of unprecedented UK rainfall in the current climate. *Nature Communications*, *8*(1), 107. https://doi.org/10.1038/s41467-017-00275-3

Tierney, J. E., Ummenhofer, C. C., & Demenocal, P. B. (2015). Past and future rainfall in the Horn of Africa. *Science Advances*, *1*(9), e1500682. https://doi.org/10.1126/sciadv.1500682

Van den Brink, H., Können, G., Opsteegh, J., van Oldenborgh, G. J., & Burgers, G. (2004). Improving 104-year surge level estimates using data of the ECMWF seasonal prediction system. *Geophysical Research Letters*, *31*(17), L17210. https://doi.org/10.1029/2004gl020610

Van den Brink, H., Können, G., Opsteegh, J., Van Oldenborgh, G., & Burgers, G. (2005). Estimating return periods of extreme events from ECMWF seasonal forecast ensembles. *International Journal of Climatology: A Journal of the Royal Meteorological Society*, *25*(10), 1345–1354. https://doi.org/10.1002/joc.1155

Wainwright, C. M., Finney, D. L., Kilavi, M., Black, E., & Marsham, J. H. (2021). Extreme rainfall in East Africa, October 2019–January 2020 and context under future climate change. *Weather*, *76*(1), 26–31. https://doi.org/10.1002/wea.3824

WFP. (2023). *Drought in the Horn of Africa: Situation update* (Technical Report). World Food Programme. Retrieved from https://reliefweb.int/report/ethiopia/drought-horn-africa-situation-update-july-2023

WMO. (2023). *2023 confirmed as hottest month on record* (Technical Report). World Meteorological Organization. Retrieved from https://public.wmo.int/en/media/news/july-2023-confirmed-hottest-month-record